IL NUOVO CIMENTO **42 C** (2019) 49
DOI 10.1393/ncc/i2019-19049-2

COLLOQUIA: SoHe3 2018

Solar perturbations transits in Mercury exosphere

V. MANGANO(1), S. ORSINI(1), A. MILILLO(1), C. PLAINAKI(2), A. MURA(1), J. M. RAINES(3), E. DE ANGELIS(1), R. RISPOLI(1), F. LAZZAROTTO(1) and A. ARONICA(1)

(1) *INAF-IAPS - Via del Fosso del Cavaliere, 100, 00133 Rome, Italy*
(2) *ASI - Via del Politecnico, 00133 Rome, Italy*
(3) *Climate and Space Sciences and Engineering Dept., University of Michigan - Ann Arbor, MI, USA*

received 28 December 2018

Summary. — The link existing between the dayside Na exospheric patterns of Mercury and the solar wind-magnetosphere-surface interactions is investigated thanks to the synergy of Earth-based observations with the THEMIS solar telescope and the in-situ measurements of the Interplanetary Magnetic Field (IMF) and proton fluxes at the magnetic cusp regions by MESSENGER. Frequently, two-peak patterns of variable intensity are observed, located at high latitudes in both hemispheres. Occasionally, Na signal is instead diffused above the sub-solar region. In a special case, the Na signal is diffused above the subsolar region, when the MESSENGER data detect the transit of two Coronal Mass Ejections (CMEs). Na emission patterns results to be clearly related to the solar wind conditions at Mercury. Hence, the Na exospheric patterns, observed from ground, could be considered as a natural monitor of solar disturbances when transiting near Mercury.

1. – Introduction

The exospheric Na emission at 589 nm, thanks to its good visibility also from the ground, is broadly used to study the tenuous neutral envelope surrounding Mercury, and to try to define clearly all the complex interactions occurring among the different parts of Mercury environment, including: surface, magnetosphere, Sun and inner heliosphere. In fact, the peculiar morphology and fast dynamics of the exosphere of Mercury is certainly linked to all these components, due to the fact that Mercury is strongly exposed to solar thermal and UV radiation and to Interplanetary Magnetic Field (IMF), and heavily bombarded by micrometeoroids and by solar wind plasma. Since the discovery of Na exosphere in the mid 80s, peculiar and recurrent exospheric patterns are observed [1]. More recently, thanks to the Earth-based observation campaign performed at the THEMIS solar telescope [2], sequences of data for many hours per day have been collected and been used to study the high dynamicity and morphology of the exosphere of Mercury through

its Na component [3-7]. Recurrent patterns can be divided into two main categories: two peaks located at high latitudes in the sub-solar region in both hemispheres, with variable intensity, often persisting for several hours, or even days; or a single peak, still located in the sub-solar region, well focused and centered in the equatorial region or spread into the illuminated part of the disk. In the first case, the peak areas approximately correspond with the magnetic cusps projection on the surface, thus supporting the idea that solar wind precipitation through these regions plays a key role in its generation. As a consequence of solar wind particles impacting the surface in these regions, the Na atoms embedded in the upper surface layer can be released. Then, the detection of IMF condition in situ during remote observations of Na exosphere becomes crucial to verify the relationship between Na exospheric pattern and planetary space weather.

2. – Analysis and Results

The synergic study of the Na exosphere through Earth-based images collected at THEMIS, together with in-situ measurements by MESSENGER instrumentation (magnetometer MAG and ion detector FIPS) during years 2011-2013, allowed us to investigate the possible correspondences of the exosphere itself with interplanetary magnetic field IMF, and with local ion populations [7]. Ten sequences of data (with more than 3 images) with good seeing conditions ($\leq 2''$) were selected. In 9 cases over 10, the bi-dimensional maps of Na exosphere above the disk of Mercury show the typical two-peak pattern, in accordance with what has been shown by [1] and [5] to be the most frequent one (Fig. 1). Only one sequence presents a different emission pattern (Fig. 2), widespread on the dayside, and occurred on September 20th 2012, as a Coronal Mass Ejection (CME) hit Mercury [8]. In Fig. 1 the upper four panels show the MESSENGER profiles vs. time as described in the caption (FIPS; MAG, and ephemeris) on June 7th 2012. Every time the S/C reached the periapsis, the MAG measurement showed a steep increase due to the crossing of the magnetopause, while in the solar wind the IMF magnitude profile is generally constant, at about 30 nT, indicating solar wind mostly undisturbed conditions. FIPS spectrograms show solar wind particles at about 1 keV. It should be noted that when IMF magnitude exceeds 25 nT we expect that reconnection may occur continuously, independently on the IMF components, that in this case are characterized by positive Bx, and By and Bz components randomly distributed around 0. In these undisturbed conditions, the planet's bow shock should stay at nominal distance from the planet (1.45 R_M [9]), reconnection should occur continuously (IMF $>$ 25 nT) and solar wind particles should regularly precipitate towards the surface through the cusps. Such plasma precipitation signatures are actually detected by FIPS when crossing the northern cusp, just at the S/C entrance inside the magnetosphere, in both the two traversals shown in Fig. 1. The bottom panel of Fig. 1 shows the corresponding 1-hour Na emission images observed by THEMIS: images show the typical two-peak patterns. Although the intensity of the two peaks is fluctuating throughout the whole time period, the general configuration appears to be quite constant. Also the other eight sequences analyzed refer to mostly undisturbed solar wind conditions, and show two peaks, so that we may infer that two-peak patterns could be the exospheric response to mostly undisturbed solar wind conditions (when IMF $>$ 25 nT at the Mercury location). Figure 2, instead, shows the case of a strong solar perturbation hitting Mercury, as it was also detected by MESSENGER. Specifically, the solar perturbation was composed by two separate CME-induced shock fronts, one just after the other, the first transiting at 09:53, and the second at 18:29 [8]. FIPS spectrograms are mostly saturated, due to the related Solar Energetic

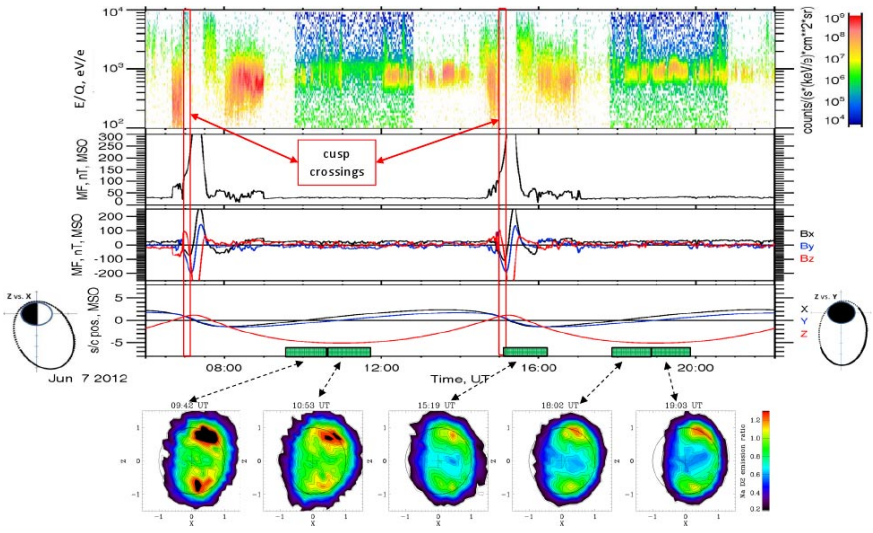

Fig. 1. – June 7th 2012 time profiles. From top to bottom: FIPS proton spectrograms (the two cusp traversals are marked by red bars), MAG magnetic field (MF) magnitude, MAG MF components (MSO), s/c ephemeris components (MSO), the 1-hour-based Na dayside patterns observed by THEMIS. At the two sides of the ephemeris plot, s/c anti-clockwise orbital paths are shown. MESSENGER data are originated from the database server AMDA, http://amda.cdpp.eu. The color scale to the right relates to an intensity index that is normalized respect to the average Na intensity profile vs. TAA, as derived by [10].

Particles event (SEP) penetrating the instrument. The MAG data indicate, at the time of the two CME transits, two abrupt jumps of the IMF magnitude (at about 10.00 and 18.30 UT) now different from the magnetopause traversals observed in the previous case. In the whole period, the IMF magnitude reaches 150 nT max, and on average ranges at about 60 to 80 nT, except for two time periods (at 12:45 to 13:20 UT) and in-between the end of the first CME and the arrival of the second one (at 17:25 to 18:30 UT). In both time periods, the IMF goes down to about 40 nT, closer to the quiet time conditions. The related Na exospheric images from THEMIS of that day are available for the whole period from 10:17 to 18:46 UT. On that day the Na emission is very diffused on the dayside, sometimes hardly showing two peaks very close to the equatorial region. The 3rd image instead, corresponding to the first IMF decrease, shows a much more evident two-peak pattern. In the 7th image, when the first CME transit vanishes, and before the second ICME arrival, only a very tenuous signal is recorded. On the contrary the last image, just when the second CME transit starts, occurs to have the most intense and diffuse pattern.

3. – Conclusions

The events shown in Figs. 1 and 2 suggest that, in condition of strongly enhanced IMF like at the occurrence of CMEs, the Na exospheric signal, induced by particle precipitation, is mainly much diffused in the equatorial region, though sometimes it exhibits two peaks pattern hardly visible and very close to the equator. On the contrary, Fig. 1 gives us the situation of IMF and Mercury exosphere interaction during quiet

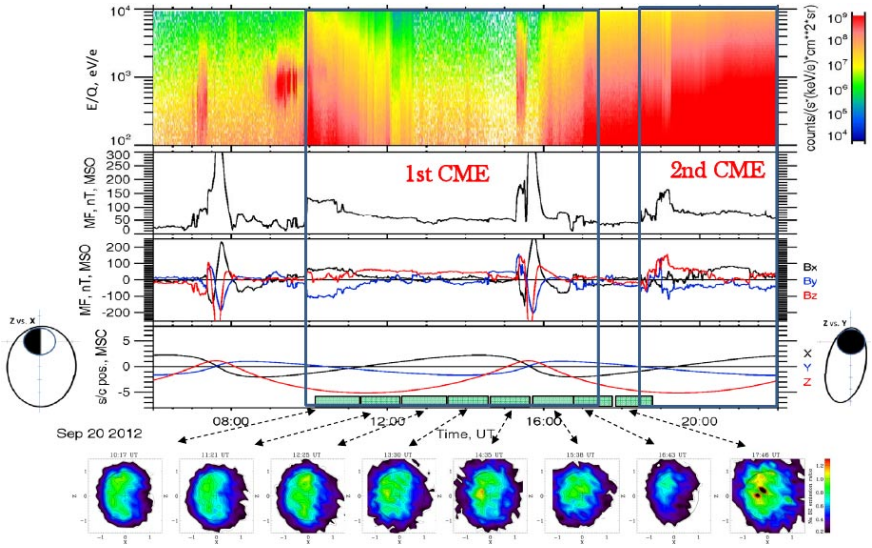

Fig. 2. – September 20th 2012 time profiles (for description see Fig. 1). The arrival of two CMEs occured at 09:53 and at 18:29.

periods, that seems to induce the well-known two-peak Na pattern. In summary, the Na exospheric emission observed in the analyzed 10 sequences database leads to the following scenario:during IMF quite conditions, reconnection occurs almost continuously as well as solar wind precipitation in the magnetic cusps, leading to the 2-peak pattern observed in the Na exospheric images from Earth-based telescopes. During intense events (like CMEs), the small gyroradius of planetary magnetosphere leads ionized particles to hit the surface also in the equatorial region, then leading to a different pattern in Na exosphere, now peaking in the equatorial sub-solar region. As a consequence, the Na exosphere of Mercury becomes a proxy of the IMF conditions in that region and may also be used as a monitor to forecast space weather conditions of the inner Solar System. Moreover, as shown by [11], CME forecast at Mercury is now possible with some hours in advance and this will allow to collect new sequences of Mercury exosphere observations during extreme events to confirm the evidenced relationship exospheric morphology and dynamics and the solar wind plasma characteristics.

REFERENCES

[1] POTTER A. E. *et al.*, *Icarus*, **181** (2006) 1.
[2] LEBLANC F. *et al.*, *Geo. Res. Lett.*, **35** (2009) 18.
[3] LEBLANC F. *et al.*, *Geo. Res. Lett.*, **36** (2009) 7.
[4] MANGANO V. *et al.*, *Planet. Space Sci.*, **82** (2013) 1.
[5] MANGANO V. *et al.*, *Planet. Space Sci.*, **115** (2015) 102.
[6] MASSETTI S. *et al.*, *Geophys. Res. Lett.*, **44** (2017) 2970.
[7] ORSINI S. *et al.*, *Scientific Reports*, **8** (2018) 928.
[8] WINSLOW R. M. *et al.*, *AGU Fall Meeting Abstracts*, (2015) SH53A-2469.
[9] WINSLOW R. M. *et al.*, *J. Geophys. Res.,Space Physics*, **118** (2013) 2213.
[10] LEBLANC F. and JOHNSON R. E., *Icarus*, **209** (2010) 280.
[11] NAPOLETANO G. *et al.*, *J. Space Weather Space Clim.*, **8** (2018) A11.